# Evidence for Trivelpiece-Gould Modes in a Helicon Discharge

D. D. Blackwell, T. G. Madziwa, D. Arnush, and F. F. Chen
*Electrical Engineering Department, University of California, Los Angeles, California 90095-1594*
(Received 23 July 2001; published 25 March 2002)

The high ionization efficiency of helicon discharges has been attributed to Landau damping and mode coupling to Trivelpiece-Gould (TG) modes. Though theory predicts the importance of TG modes, they have rarely been seen. Here they were detected directly by measuring their radiofrequency current with a J-dot probe, thus supporting the contention that TG modes play a role in these enigmatic plasma sources.

DOI: 10.1103/PhysRevLett.88.145002 PACS numbers: 52.80.–s

Helicon (H) discharges, in which radiofrequency (rf) energy is absorbed by bounded whistler waves, have been studied intensively because of their ability to generate high plasma densities at low pressures and rf powers, with applications to semiconductor processing and space propulsion. Shamrai *et al.* [1] have proposed that the efficiency of the absorption mechanism is not due to Landau damping, as surmised by Chen [2], but to coupling to Trivelpiece-Gould (electron cyclotron) modes, which, being quasielectrostatic, are rapidly absorbed as they propagate inward from the radial boundary. Computations by Kamenski and Borg [3], Enk and Kraemer [4], Mouzouris and Scharer [5], Park *et al.* [6], and Shamrai and Shinohara [7] all predict that rf power is absorbed more efficiently by Trivelpiece-Gould (TG) modes than by helicon waves. The HELIC code of Arnush [8] yields plasma loading resistances in agreement with experiment [9]. Being the only code available to us, HELIC was used for this work. Direct detection of TG modes is difficult because these modes tend to be localized in an irresolvably thin layer near the surface. However, at magnetic fields below about 50 G, TG modes extend far into the interior of the discharge, and their effect on the wave shapes should be detectable.

Experiments were done in the 10 cm diam, 110 cm long device shown in Fig. 1. To facilitate comparison with theory, the simplest antenna was used: an azimuthally symmetric ($m = 0$) loop, shown in Fig. 2a. A Faraday shield (Fig. 2a) was used to minimize capacitive coupling, which could cause plasma asymmetries [10]. Diagnostics included Langmuir probes, magnetic ("$B$-dot") probes for $B_z$ and $B_\theta$ of the wave, and a new rf current probe, to be described later. The antenna was located 15 cm from a conducting end plate and 30 cm from the midplane port, where most of the data were taken. The discharge was operated in 2–3 mTorr of argon with 0.8–1 kW of 11 MHz power and a dc field $\mathbf{B}_0\hat{\mathbf{z}}$ of 25–60 G. This range of parameters gave stable discharges of density $n = (2\text{–}10) \times 10^{11}$ cm$^{-3}$ in which the TG mode was predicted [11] to have similar radial wavelengths and thus be detectable. This narrow window is illustrated in the dispersion relation of Fig. 3 for coupled H-TG modes [11] at a density of $4 \times 10^{11}$ cm$^{-3}$. At a given $k$, such as that shown by the dotted line, the two values of $\beta$ corresponding to the H and TG modes are close only for a small range of $B_0$ around 30 G. At fields as high as 300 G, $\beta_{\mathrm{TG}}$ would be so large that the TG mode would be confined to a thin edge region. Initial measurements of $|B_z|$ showed little evidence of the H-wave profile change caused by the presence of a TG mode. This effect could be amplified, however, by measuring the rf current $J_z$ rather than the rf magnetic field $B_z$. That $J_z$ is more sensitive to the TG mode than $B_z$ can be seen from simple helicon theory. Both the H and TG waves satisfy [11]

$$\mu_0 \mathbf{J} = \nabla \times \mathbf{B} = \beta \mathbf{B}, \qquad J_z = (\beta/\mu_0) B_z, \quad (1)$$

where

$$\beta_{\mathrm{TG,H}} = \frac{k}{2\delta}\left(1 \pm \sqrt{1 - \frac{4k^2\delta^2}{k_s^2}}\right), \quad (2)$$

$\delta = \omega/\omega_c$, $k_s = \omega_p/c$, and $k$ is the axial wave number. Here $\beta_{\mathrm{TG}}$ is the upper (+) root and $\beta_{\mathrm{H}}$ the lower (−) root, so that their ratio is always $>1$ (cf. Fig. 3). Equation (1) indicates that if both modes have the same $|B_z|$, the TG mode will have larger $|J_z|$ by the ratio $\beta_{\mathrm{TG}}/\beta_{\mathrm{H}}$. This is evident in the theoretical profiles shown in Fig. 4a as well as the measured profiles of Figs. 4b and 4c, where the outer peak due to the TG mode can be seen only in $|J_z|$.

To measure $J_z$, a miniature J-probe (essentially an rf Rogowski coil) was made and carefully calibrated. The probe consists of 150 turns of coated wire wound poloidally on an insulating coil form, resulting in a ring of ~4 mm i.d. and ~9 mm o.d. To cancel the toroidal components of the coil current, a return loop was wound in a groove on the inside, as shown in Fig. 2b. The windings were covered with a copper Faraday shield with a toroidal slit. The

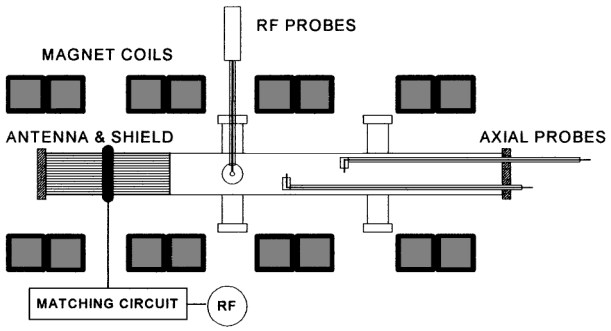


FIG. 1. Diagram of the apparatus.

 © 2002 The American Physical Society 

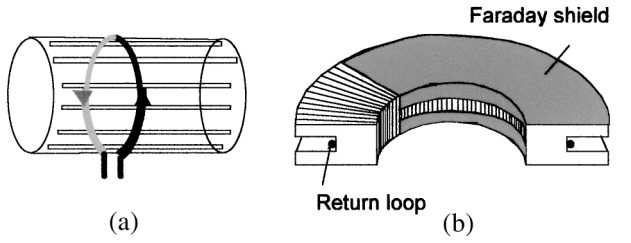


FIG. 2. (a) $m = 0$ antenna and Faraday shield. (b) Schematic of J-dot probe.

coil was mounted on a 3.2-mm o.d. stainless steel tube, and the twisted-pair leads were threaded through an inner shield consisting of an 0.8-mm diam hypodermic needle. The leads were connected to a 1-1 balun transformer, and the unbalanced signal then passed through a bandpass filter to a digital oscilloscope. The probe was deployed in the port 30 cm downstream from the antenna (Fig. 1). The sensitivity of the probe was measured by passing a known rf current in a wire along the major axis of the torus. Rejection of electrostatic signals was tested by immersing the coil in a mercury bath and applying a known rf voltage to the mercury. The pickup per volt applied was 0.4 mV, compared with a typical $J_z$ signal of 10–30 mV. The most difficult task was to eliminate the B-dot signal from $B_z$ fields passing through the torus and imperfectly canceled by the return loop described above. This effect was checked by placing the coil in a Helmholtz coil which produced a known $B_z$ field. The pickup from a 1-G $B_z$ field at 11 MHz was only 0.2 mV. These sources of error added to $<10\%$. Finally, the J-probe was tested inside the pulsed helicon discharge. Rotating the probe 180° gave a reversed signal to within 10°. Rotating it 90° yielded $J_\theta$ instead of $J_z$, with a completely different radial profile, as shown in Fig. 5. Withdrawing the probe into the port arm dropped the signal by 90%. $B_z$ pickup was tested by plugging the opening in the J-probe with a ceramic disk. The signal was reduced by only a factor of 2–4; this was attributed to displacement current through the ceramic. Of 20 coils constructed, only two passed all of these tests.

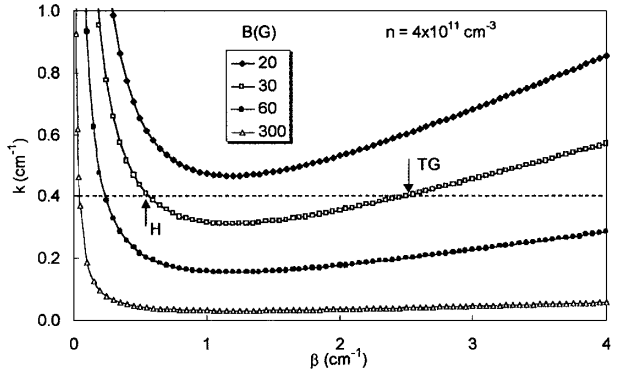


FIG. 3. A $k$-$\beta$ plot of Eq. (2) for $f = 11$ MHz, $n = 4 \times 10^{11}$ cm$^{-3}$, and various fields $B_0$.

Inserting the probe through the center of the plasma necessarily disturbs the discharge. Hence, in the graphs shown, data on both sides of the axis were averaged to produce a symmetric pattern to compare with theory. Data could be reproduced from month to month. The theoretical curves were computed with the HELIC code of Arnush [8,12], incorporating H-TG mode coupling; electron collisions with neutrals and ions at $T_e = 3$ eV and $p = 3$ mTorr; the radial density gradient; and antenna

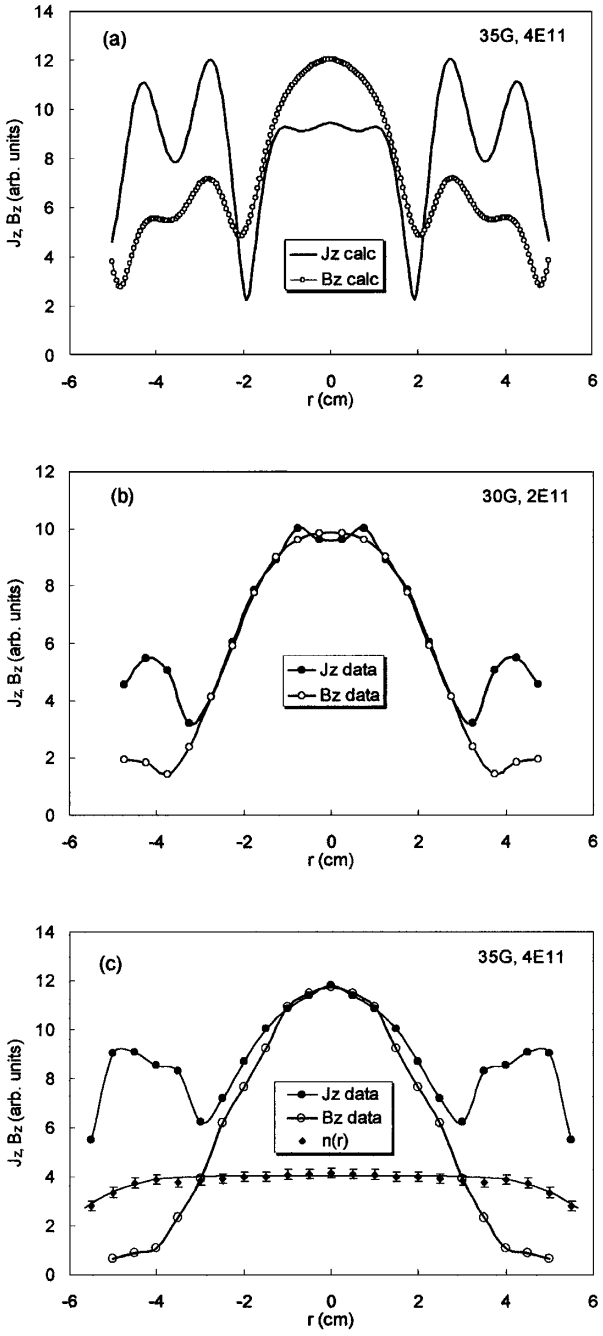


FIG. 4. Typical radial profiles of $|B_z|$ (○) and $|J_z|$ (●) as (a) calculated and (b),(c) measured. In (c) a typical density profile $n(r)$ is also shown, together with the curve used to model it.

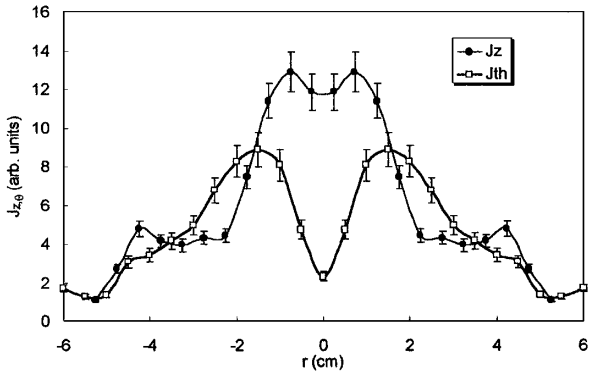


FIG. 5. Magnitudes of $J_z(r)$ and $J_\theta(r)$ obtained by rotating the J-probe 90°, showing the zero crossing in $J_\theta$. Error bars indicating typical shot-to-shot variation as shown here but omitted in other graphs for clarity.

coupling, including the effects of image currents on the end plate. For a radially uniform density, the Shamrai Bessel function solutions [1] are used, whereas the nonuniform density differential equations are solved, and the H and TG modes are distinguished by their behavior near the axis [11]. Instrumental resolution was included by averaging the curves over the i.d. of the J-probe. The computations were for an infinitely long plasma with no axial gradients. Tests were made of the effect of the conducting end plate near the antenna. Imposing the boundary condition $J_z = 0$ at the end plate had a noticeable affect on the $J_z$ profiles but did not change their general character. The boundary condition $\mathbf{E}_\perp = 0$ gave less reasonable results. Ignoring reflections from the ends gave the best agreement.

Preliminary measurements given elsewhere [13] verified that the discharge was operating in the normal helicon regime. Profiles of waves $B_z$ and $B_\theta$ at 100 G and above exhibited the classical Bessel function shape of simple H waves [14]. That these $m = 0$ profiles were symmetric was checked with two probes 90° apart in azimuth; this was not the case with $m = 1$ waves generated by a helical antenna, presumably because of the difficulty in constructing a helical Faraday shield of sufficient accuracy. Phase measurements of $B_z$ along the axis showed propagation with an axial wavelength agreeing with theory. Figure 4c shows a typical density profile, which is uniform except for a small roll-off at the edge. The electron temperature is ~3 eV; it affects only the collisional term in the computations.

Figure 6 shows the $|J_z|$ profiles at 30 G and three densities, as compared with curves calculated with the HELIC code with and without the TG mode included. With collisions, there can be no solution with $E_z = 0$ representing the simple H mode; the "no TG" curve is the component that behaves like a Bessel function near the axis. In each case, it is seen that the data show the "wings" due to the presence of the TG mode which are not present with the H mode alone. The J-probe is unable to resolve the fine

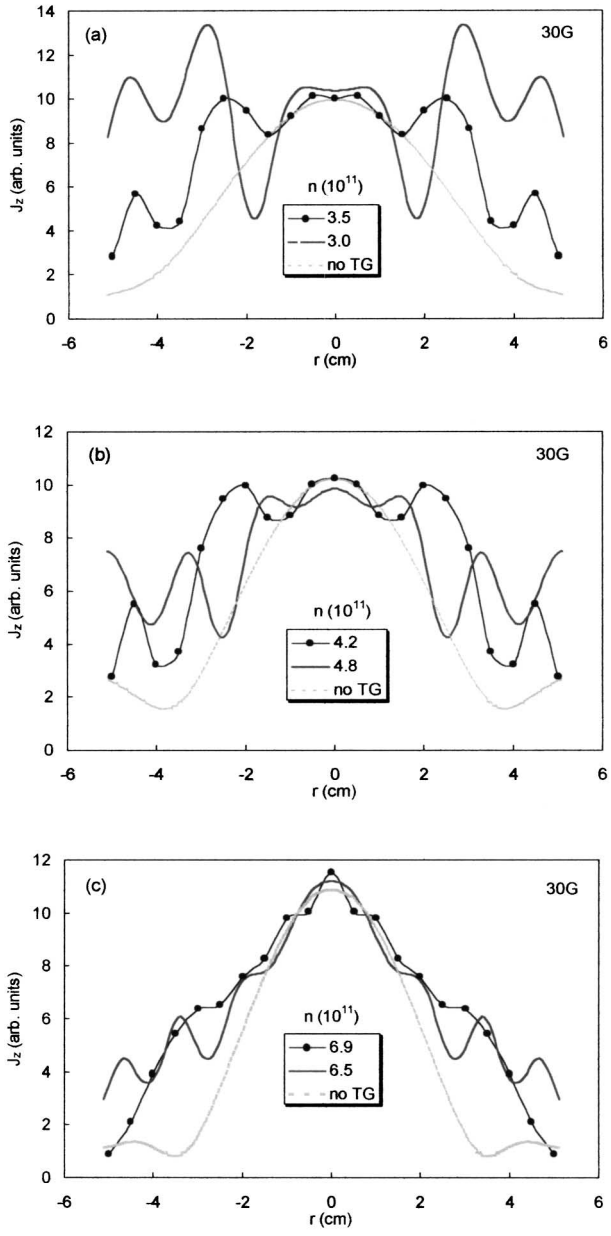


FIG. 6. Radial profiles of rf current $|J_z|$ at 30 G and various densities (in $cm^{-3}$) as measured (●), as predicted by theory (———), and as calculated from simple helicon theory without the TG mode (– – – –).

structure of these wings, but they are clearly present. The magnitudes and positions of the TG peaks could not always be reproduced by the theory, partly because of equilibrium profile effects not included in the calculations, and partly because of imperfections in the J-probe, as explained in the calibration procedures. In some cases adjusting the density in the computation improved the fit. This is reasonable because (a) the density at the probe port can differ from that under the antenna, depending on the location of the downstream density peak [15], and (b) densities found from saturation ion currents can be in error by as much as 100% [16]. Note that at $n = 6.9 \times 10^{11}$ $cm^{-3}$ destructive

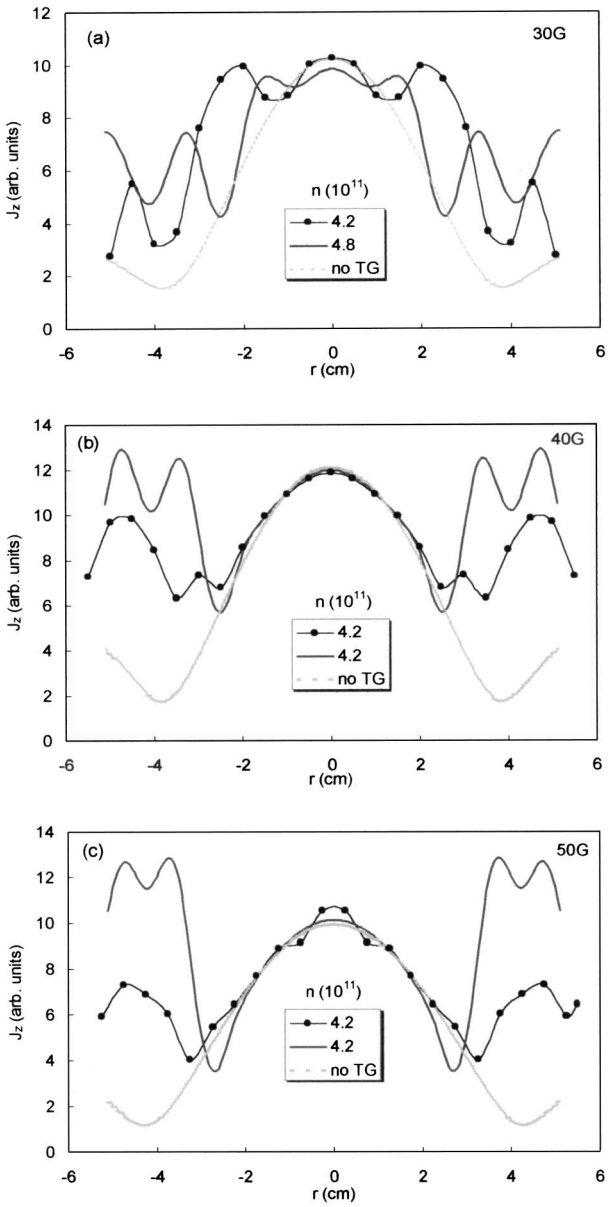


FIG. 7. Same as Fig. 6 but with varying $B_0$ at a constant density.

interference between the H and TG modes has suppressed the TG wings; this effect is seen in both the data and the theory. Figure 7 shows the $|J_z|$ profiles for 30, 40, and 50 G at $n = 4.2 \times 10^{11}$ cm$^{-3}$. The presence of the TG mode is evident in each case. As $B_0$ is increased, the H mode dominates near the axis, and this is manifested by the good agreement among the data and the two theoretical curves there. The TG mode was purported to have been seen by Lho *et al.* [17], but those B-dot data did not show the wings that we could see only with the J-dot probe.

The energy deposition mechanism in helicon discharges is unusual and has been disputed. Electron mass effects giving rise to TG modes had been neglected in early helicon theories, but once included, they yield values of loading resistance agreeing with experiment. Up to now, TG modes had not been observed directly. This work provides evidence for their existence and differs from all previous work on rf discharges by the use of an rf current probe. Absorption by TG modes has not been measured; for this we depend on detailed calculations [3–8], which predict that, at the higher magnetic fields used in practice, they would be too localized to be detected but would nonetheless greatly affect the energy absorption.

The authors thank J. D. Evans for suggesting the construction of a J-dot probe.

[1] K. P. Shamrai and V. B. Taranov, Plasma Sources Sci. Technol. **5**, 474 (1996).
[2] F. F. Chen, Plasma Phys. Controlled Fusion **33**, 339 (1991).
[3] I. V. Kamenski and G. G. Borg, Comput. Phys. Commun. **113**, 10 (1998).
[4] Th. Enk and M. Kraemer, Phys. Plasmas **7**, 4308 (2000).
[5] Y. Mouzouris and J. E. Scharer, Phys. Plasmas **5**, 4253 (1998).
[6] B. H. Park, N. S. Yoon, and D. I. Choi, IEEE Trans. Plasma Sci. **29**, 502 (2001).
[7] K. P. Shamrai and S. Shinohara, Phys. Plasmas **8**, 4659 (2001).
[8] D. Arnush, Phys. Plasmas **7**, 3042 (2000).
[9] D. G. Miljak and F. F. Chen, Plasma Sources Sci. Technol. **7**, 61 (1998).
[10] D. D. Blackwell and F. F. Chen, Plasma Sources Sci. Technol. **6**, 569 (1997).
[11] F. F. Chen and D. Arnush, Phys. Plasmas **4**, 3411 (1997).
[12] D. Arnush and F. F. Chen, Phys. Plasmas **5**, 1239 (1998).
[13] D. D. Blackwell, Ph.D. thesis, UCLA, 1999.
[14] M. Light and F. F. Chen, Phys. Plasmas **2**, 1084 (1995).
[15] D. G. Miljak and F. F. Chen, Plasma Sources Sci. Technol. **7**, 537 (1998).
[16] F. F. Chen, Phys. Plasmas **8**, 3029 (2001).
[17] T. Lho, N. Hershkowitz, J. Miller, W. Steer, and G. H. Kim, Phys. Plasmas **5**, 3135 (1998).